中国激光

鲜红斑痣病灶结构及其光学成像方法在血管靶向光动力治疗中的研究进展

刘一荻[1,2]，陈德福[3]，曾晶[2]，邱海霞[2**]，顾瑛[2,3,4*]

[1]解放军医学院，北京 100853；

[2]解放军总医院第一医学中心激光医学科，北京 100853；

[3]北京理工大学医学技术学院，北京 100081；

[4]中国医学科学院精准激光诊疗创新单元，北京 100730

摘要 鲜红斑痣(port wine stains，PWS)是最常见的先天性皮肤微血管病变之一，PWS 的病因是皮肤真皮层由浅至深的毛细血管畸形扩张。通常表现为面颈部粉色、红色和紫色斑片，随着年龄的增加，其逐渐加深和增厚，严重影响患者的生活质量。血管靶向光动力疗法（vascular targeted photodynamic therapy，V-PDT）可以选择性破坏病变血管，是目前国内治疗 PWS 的首选方法。V-PDT 疗效与 PWS 病灶结构密切相关。PWS 的病灶结构可通过活检或者无创光学诊断设备获取，主要包括表皮层黑色素含量、皮肤厚度及血管管径、深度和形态等。总结了目前常用的无创在体光学成像技术在 PWS 诊疗中的应用现状及 PWS 病灶结构特点对 V-PDT 疗效的影响，旨在为 V-PDT 精准及个性化治疗 PWS 提供参考。

关键词 医用光学；鲜红斑痣；血管靶向光动力疗法；病灶结构；疗效

中图分类号 R758.5 **文献标志码** A **DOI**：10.3788/CJL202249.1507102

1 引 言

鲜红斑痣(port wine stains，PWS)又称为“葡萄酒样痣”，是最常见的先天性皮肤病之一，发病率为 0.3%～0.5%[1-3]。PWS 以真皮内存在多量畸形扩张的毛细血管为特征[4]，畸形扩张血管的管径通常为 10～150 μm，在增厚型 PWS 中甚至可达 500 μm[5-7]。PWS 的临床表现为单侧(偶为双侧)皮肤呈现粉红、暗红或紫红色斑片，好发于头皮、面、颈部等外露部位。随着年龄的增长，PWS 病变颜色逐渐加深，病灶增厚，并且约有 65%患者的病灶在 50 岁之前会明显增生并产生多量结节样改变，创伤后易出血[8]，严重影响患者面容并降低其生活质量。

PWS 的进展性和毁容性给患者带来了巨大的身心负担[9]，患者迫切需要临床治疗。治疗 PWS 的关键是选择性地祛除扩张畸形的毛细血管网而不损伤表皮和真皮深层。在早期，同位素放射性治疗和冷冻等非选择性治疗方法被用于 PWS 的治疗，但疗效差、副作用大，会导致病灶明显的瘢痕及色素异常，目前上述治疗方法已经被淘汰。脉冲染料激光(pulsed dye laser，PDL)在国外一直被认为是治疗 PWS 的金标准[10-11]，该波长(585 nm 或 595 nm)激光可被 PWS 畸形血管内的血红蛋白选择性吸收，产生凝固变性，血管机化闭塞，从而畸形血管遭到破坏。在治疗 PWS 时，大多数患者病损颜色的消退程度可达 50%以上，但是有多项研究表明，约有 20%的 PWS 患者对 PDL 治疗不敏感[12-16]，且在 PDL 治疗后 10 年内，会出现原本已治疗褪色的病灶区返红的情况[17]。血管靶向光动力疗法（vascular targeted photodynamic therapy，V-PDT)[18]于 1991 年由解放军总医院激光医学科的顾瑛首先提出，其有效性和高安全性使其成为目前国内 PWS 治疗的首选方法[19-22]。有学者将 PWS 患者同一部位的病灶一分为二，一半接受 PDL 治疗，一半接受 V-PDT 治疗，结果表明，V-PDT 的治疗效果显著优于 PDL[23]。

尽管 V-PDT 在治疗 PWS 中展现了显著优势，但仍有部分患者疗效不佳，甚至部分患者无显效。PWS 病变结构十分复杂，病灶结构存在显著的部位和个体差异[24-25]，从而导致了 V-PDT 疗效存在明显的差异性。而在临床诊疗中，由于缺少客观诊断标准，医生主要根据患者 PWS 病变的临床表征(如颜色、是否增厚等)对患者的病情进行预判，进而制定治疗方案，但这

收稿日期：2022-01-06；**修回日期**：2022-01-30；**录用日期**：2022-02-17

基金项目：国家自然科学基金(61835015)、2021 年度全国学会期刊出版能力提升计划(产业发展服务-27)、解放军总医院大数据项目(2019MBD-011)、中国医学科学院医学与健康科技创新工程项目基金(2019-I2M-5-061)

通信作者：*guyinglaser301@163.com；**qiuhxref@126.com

些临床表征并不能客观反映 PWS 复杂的病灶结构特点。例如 PWS 病变颜色的深浅不仅与畸形血管的扩张程度有关[26]，还与表皮层黑色素含量、表皮层厚度及血管深度和形态等因素有关[27]。因此，了解 PWS 病灶结构特点与 V-PDT 疗效之间的关系，并通过无创光学诊断设备获取 PWS 病灶结构信息，对于临床上判断病变严重程度、制定诊断标准、优化治疗方案以及判断预后等具有重要意义。

本文综述了目前可用于 PWS 病灶结构及功能成像的无创光学诊断设备，总结了 PWS 病灶结构与 V-PDT 疗效之间的关系，以期对临床提高 V-PDT 疗效有所裨益。

2 V-PDT 治疗 PWS 的原理

V-PDT 治疗 PWS 的原理：静脉注射光敏剂后，光敏剂立即在血液中形成浓度高峰，此时选择性采用特定波长激光照射病变部位，病变部位的毛细血管网因富含光敏剂，发生Ⅱ型光敏氧化反应，生成具有细胞毒性的单线态氧（singlet oxygen，$^1O_2$），导致病变靶血管的破坏[28-30]。正常表皮层因光敏剂含量低而不受损伤，位于真皮深层的营养血管由于激光穿透深度限制而不发生光动力反应[31]。

如图 1 所示，在 V-PDT 治疗过程中，激光作为治疗光源首先需要穿过表皮层才能到达真皮浅层的病变血管，因此黑色素作为表皮层中的主要光吸收体，其含量会影响激光到达病变血管处的光子量；其次，表皮层的厚度对光的穿透也有影响。除了表皮层外，真皮内血管管径、位置、形态等都会影响病变结构的组织光学特性，进而影响光在 PWS 组织中的分布，从而影响 V-PDT 的效果。此外，血液作为真皮层的主要光吸收体，其含量（血流灌注量）也会影响光在皮肤组织中的分布。

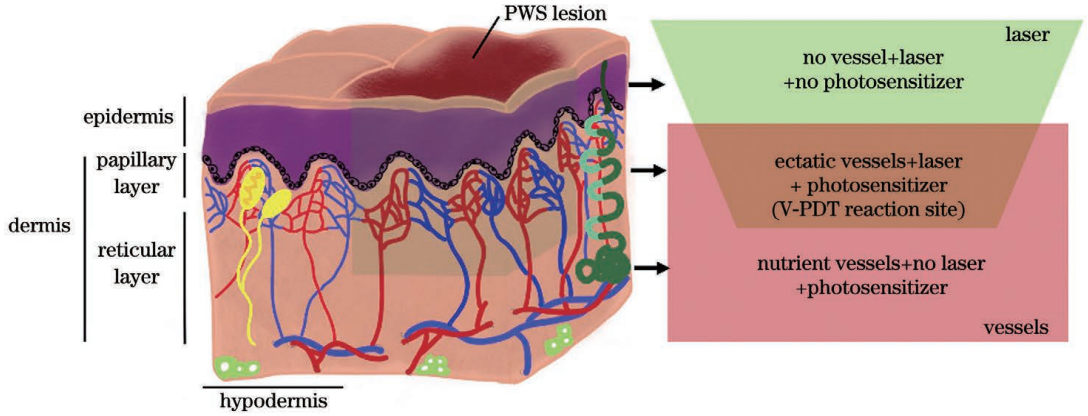

图 1 V-PDT 治疗 PWS 的原理

Fig. 1 Principle of V-PDT used for treating PWS

3 PWS 在体结构成像常用的新型无创光学技术

传统的病理活检可以获取 PWS 的病理结构，但其为有创，会遗留瘢痕，不宜反复操作，因此急需发展新型无创的光学技术。随着光学技术的发展，如表 1 所示，目前有以下较为成熟的四种光学技术可获取 PWS 病灶结构信息。此外，本节还介绍了可获取血

表 1 可获取 PWS 病灶结构的光学设备

Table 1 Optical modality for obtaining PWS lesion structure

Imaging method	Modality	Observation	Ref.	Advantage	Limitation
Structural imaging	OCT	Epidermis thickness, vascular diameter/depth	[32-35]	Non-contact imaging, quick imaging, high resolution	Shallow imaging depth
	RCM	Vascular diameter/depth	[36-37]	Fast imaging, high resolution	Being sensitive to motion, shallow imaging depth
	Dermoscope	Vascular morphology	[38-39]	User-friendliness	Two-dimensional imaging, shallow imaging depth
Functional imaging	PAI	Melanin, vascular diameter/depth/morphology	[24,40-44]	Deep imaging depth (>1 mm)	Contact measuring
	ODT/OCTA	Epidermis thickness, vascular diameter/depth/morphology	[45-48]	Non-contact imaging, quick imaging, high resolution	Shallow imaging depth
	LDI	Blood perfusion	[49-52]	Mature technique	Two-dimensional imaging
	LSI	Blood perfusion	[53-54]	Fast imaging	Two-dimensional imaging

Note: RCM, reflectance confocal microscopy; PAI, photoacoustic imaging; OCT, optical coherence tomography; ODT, optical Doppler tomography; OCTA, optical coherence tomography angiography; LDI, laser Doppler imaging; LSI, laser speckle imaging

流灌注量的两种光学技术。血流灌注量可反映血管数量、管径、深度等多种信息，在此一并讨论。

3.1 光学相干层析成像

光学相干层析成像（optical coherence tomography，OCT）是一种可对生物组织浅表微结构进行高分辨成像的光学新技术，被称为“光活检（optical biopsy）”[55]。OCT 技术在血管成像上还有许多功能性拓展。例如光学多普勒层析成像（optical Doppler tomography，ODT）系统和光学相干断层扫描血管成像（optical coherence tomography angiography，OCTA），这两者通过算法可以有效地将血管与其他微结构区分开[56-57]。

2010 年，Zhao 等[32]首次使用 OCT 成功观察并定量提取了 41 例位于面颈部的 PWS 皮肤的平均表皮层厚度，OCT 的图像如图 2（a）所示。2012 年，Zhou 等[33]使用 OCT 检测并获取了兔耳微血管的管径和深度信息，与金标准病理结果进行对比，结果无统计学差异，说明 OCT 获取的血管结构信息具有可靠性。2014 年，Zhen 等[34]用 OCT 获取了 PWS 的血管直径和深度信息。2018 年，王成铭[35]用 OCT 获取了 PWS 的表皮层厚度等信息。以上均表明 OCT 可以进行 PWS 病理结构信息的获取。在 OCT 功能成像上，2002 年，Zhao 等[58]使用 ODT 获得了 PWS 和正常皮肤的血管三维图，能够较清晰地观测到 PWS 中的畸形血管层及血流分布等，如图 2（e）所示。2016 年，Latrive 等[45]采用 ODT 定量测量了一名 PWS 患者的病变血管的平均管径和深度。2018 年，Waibel 等[46]使用 OCTA 系统首次检测并量化提取了 28 名 PWS 患者的不同粗细的血管在皮肤中不同位置处的分布情况。2020 年，Liu 等[47]应用 OCTA 观察了三名病灶位于面部的 PWS 患者并进行了高分辨的三维血管成像，如图 2（f）所示。此外，该研究还提供了血管深度和血管管径等信息。2021 年，Mehrabi 等[48]使用 OCTA 观察了粉红型、红型和紫型 PWS 患者的血管情况，并总结了各型血管位置和管径的特点。以上结果均显示，ODT/OCTA 可以获取 PWS 血管形态、管径和深度。

OCT/ODT/OCTA 可以获取表皮层厚度及血管管径和位置。此外，功能性 OCT 成像 ODT/OCTA 还可以获取血管形态，进行三维成像。但是，OCT/ODT/OCTA 均是基于纯光学成像方式，随着成像深度的加深，空间分辨率会急速下降，在皮肤中的成像深度不足 1 mm。但是大多数 PWS 平均病变血管深度为 300～600 μm[59]，故 OCT 及其相关扩展功能在 PWS 病灶结构检测方面具有良好应用前景。

3.2 光声成像

光声成像（photoacoustic imaging，PAI）技术是基于光声效应发展而来的在体无损成像技术[60]。它结合了纯光学成像的高对比度和纯超声成像的高穿透深度，可以实现类似超声的深层组织成像（成像深度＞1 mm），还能得到类似 OCT 的高分辨率[61]。

2002 年，Viator 等[40-41]使用 PAI 探测了一名 PWS 病灶位于左上肢的患者，其病灶血管的深度为 310～570 μm，表明 PAI 可以无创获取病变血管的深度信息。2008 年，Kolkman 等[42]使用 PAI 对三名病灶位于面颈部的 PWS 患者进行检测和血管的三维成像，并获取了病变血管层的厚度和深度信息，结果显示，三名患者的血管层厚度和深度信息具有显著个体差异性。2012 年，Yuan[24]选取 4 名 PWS 患者进行了 PAI 血管三维成像，分别提取了平均（最大）血管管径、平均（最大）血管深度等信息。2021 年，如图 2（d）所示，Ma 等[43]使用 PAI 对 PWS 的三维血管结构进行了成像，还测量了 PWS 患者的表皮层厚度及血管管径和深度等。2022 年，Wang 等[44]也进行了相关研究。以上研究均说明 PAI 可用于 PWS 结构信息的获取。

PAI 技术可以获取 PWS 病灶结构的表皮层黑色素含量、表皮层厚度及血管管径、深度和形态等信息，不过目前 PAI 在 PWS 的临床应用上还处于初步探索实验阶段，且 PAI 检测速度慢、耗时久，需要将探头与皮肤紧密接触，若患者皮肤受损，难以检测。

3.3 反射式共聚焦显微镜

反射式共聚焦显微镜（reflectance confocal microscopy，RCM）也是临床常用的皮肤诊断设备，其采用低功率密度近红外激光水平扫描皮肤，通过收集背向散射光进行成像[62-65]。

2010 年，Astner 等[36]采用 RCM 检测了包括 PWS 在内的多种良性血管疾病，发现 PWS 真皮浅层有许多畸形、扭曲、扩张的血管，如图 2（b）所示，血管管径分布从 75 μm 到远大于 100 μm，通常位于真皮上乳头层，而正常血管的平均管径为 17 μm[66]。2014 年，Ren 等[37]通过使用 RCM，观察了血管深度和管径的变化，评估了具有不同脉冲时间间隔的 PDL 对 PWS 治疗疗效的影响，显示 RCM 可应用于 PWS 诊治上。

RCM 可观测到皮肤血管并获取其管径、深度信息，但是 RCM 成像对振动或移动非常敏感，故在好动型患者（如儿童等）检测上受限。此外，其成像的深度浅（200～350 μm），只能对浅层病灶结构进行成像且仅能提供二维信息。

3.4 皮肤镜

皮肤镜（dermoscope）又称皮表透光显微镜，是一种可以放大数十倍乃至数百倍并可以消除皮肤表面反射光的检测设备[67]。皮肤色素和血管是其观察的两大主要对象，目前已在临床上广泛应用。

皮肤镜可观察到 PWS 病变血管形态，已有多项研究将其与 PDL 疗效相关联[38-39]。1997 年，Motley 等[38]用皮肤镜观察 15 名 PWS 患者的血管形态。如

图 2(c)所示，研究者将 PWS 血管的形态分为三型：I 型，表面的、弯曲的、扩张的毛细血管末端袢（斑点状，blobs）；II 型，扩张的、水平的血管网（戒指状，rings）；III 型，混合型，包含 I 和 II 型。Motley 等[38,68]发现，I 型患者的 PDL 疗效最好，III 型其次，II 型最差。Sevila 等[39]用皮肤镜也发现了这一现象。

虽然皮肤镜使用方便、成像快，但是其成像深度有限，不能完整反映 PWS 病灶的整体情况且皮肤镜下的 PWS 血管形态表现不具有规律性，目前皮肤镜在 PWS 的临床应用上仍较少。

3.5 激光多普勒成像和激光散斑成像

激光多普勒成像（laser Doppler imaging，LDI）是目前较常见的非介入性组织血流监测技术，其测量原理是基于光学多普勒频移效应、光混频原理及随机信号处理技术[51]。LDI 目前已经被应用于临床皮肤血流量的监测，可对 PWS 病灶区域的血液灌注量进行快速测定。激光散斑成像（laser speckle imaging，LSI）是一种基于激光散斑现象的非接触式血流光学成像方法[69]。

1996 年，Troilius 等[49]使用 LDI 观察了 13 例 PWS 患者在 PDL 治疗前后的血流灌注量的改变，发现 9 例患者治疗后的血流灌注量升高。2015 年，Mermod 等[51]使用 LDI 定量评估了 PDL 治疗 20 例 PWS 患者的疗效。如图 2(g)所示，2016 年，Chen 等[52]使用 LDI 观察了 PWS 患者在 V-PDT 治疗过程中血流灌注量的变化。在 LSI 的应用上，2009 年，Huang 等[53]发现，经 PDL 治疗后血流灌注量下降的病灶区的疗效佳。2015 年，Yang 等[54]也发现血流灌注量与 PDL 疗效具有相关性。2016 年，如图 2(h)所示，Chen 等[70]联合使用 LDI 和 LSI 测量了 PWS 区域的血流灌注量，发现二者的测量值具有线性关系。

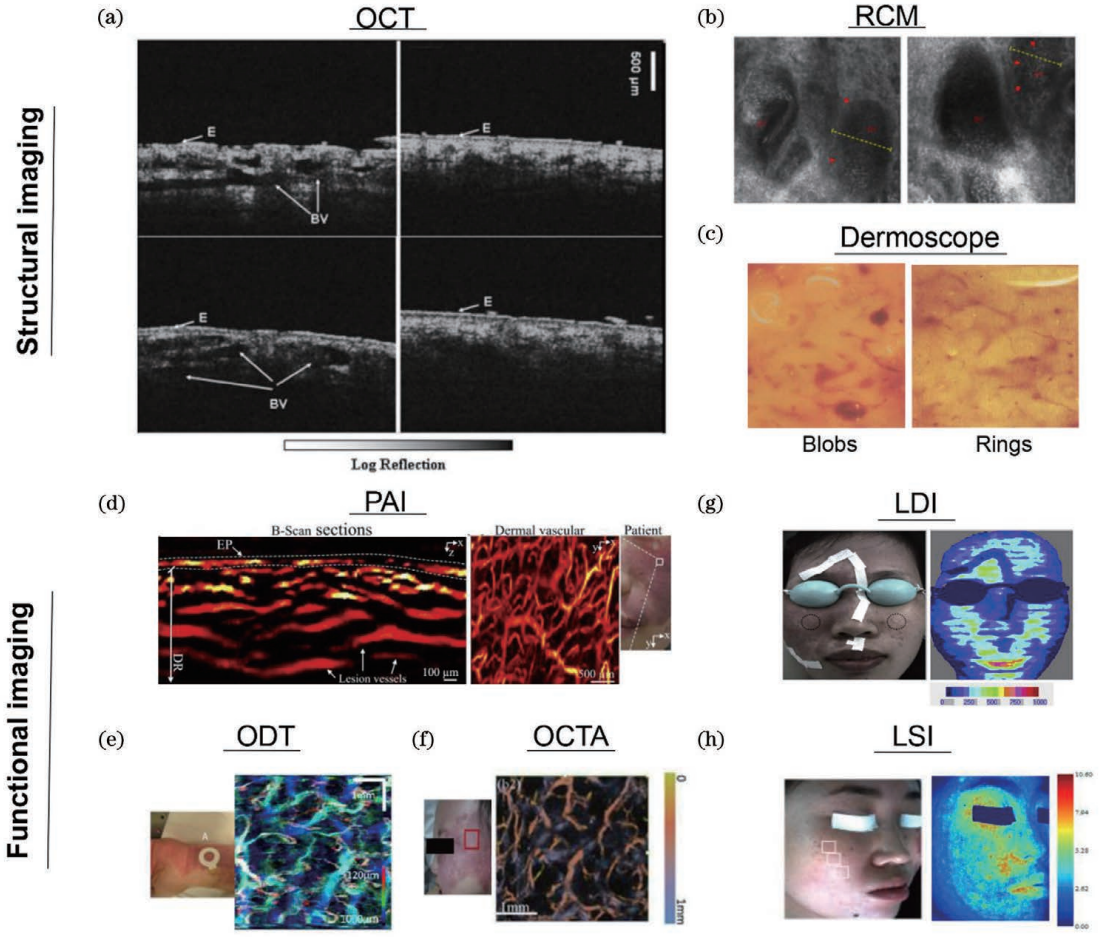

图 2 常用光学设备对 PWS 的成像结果。(a)OCT[32]；(b)RCM[36]；(c)皮肤镜[38]；(d)PAI[43]；(e)ODT[58]；(f) OCTA[47]；(g)LDI[52]；(h)LSI[70]

Fig. 2 Imaging results of PWS under common optical imaging equipment. (a) OCT[32]; (b) RCM[36]; (c) dermoscope[38]; (d) PAI[43]; (e) ODT[58]; (f) OCTA[47]; (g) LDI[52]; (h) LSI[70]

以上研究说明，LDI 和 LSI 二者均可获取 PWS 区域的血流灌注信息，且血流灌注量与疗效具有相关性。但是，LDI 和 LSI 在 PWS 成像上的分辨率低且仅能提供二维信息[52,70]。

4 PWS 病灶结构对 V-PDT 疗效的影响

PWS 病灶结构特点是影响 V-PDT 疗效的关键

因素，包括 PWS 病变部位的表皮层黑色素含量、表皮层厚度以及真皮病变血管管径、深度、形态和血流灌注量等，本部分将介绍这些因素与 V-PDT 疗效的具体关系。

4.1 表皮层黑色素含量

皮肤颜色主要取决于表皮中的黑色素含量，不同颜色皮肤因黑色素含量差异而具有不同的光学吸收系数，从而影响组织中的入射光分布。对 V-PDT 治疗 PWS 时的浅色和深色皮肤吸收系数进行数学仿真，结果发现，深色皮肤治疗中产生的 $^1O_2$ 少；而浅色皮肤的表皮色素含量较深色皮肤少，对激光的吸收较少，更多的激光被血管中的光敏剂吸收，因此产生的 $^1O_2$ 较深色皮肤多[71]。儿童患者由于累计照射紫外线较少，表皮的黑色素含量较成年人低[72]，血管中光敏剂吸收的激光较多，这也能部分解释 PWS 儿童患者的 V-PDT 疗效优于成年人的原因[73-74]。上述研究结果表明，表皮层黑色素含量越高，到达病变血管的光子量越少，从而降低 V-PDT 疗效。

4.2 表皮层厚度

表皮层是皮肤的最外层，是人体的一道天然屏障，能够有效阻止外来物质的透皮传输。在理论上，表皮层越厚，对光照射下皮肤的折射率和吸收率的影响越大，进入真皮层到达病变血管的光子量会降低，从而影响治疗效果。尽管全身各处的皮肤在结构上保持一致，但表皮层的厚度随着年龄和解剖部位的不同而有所差别。

婴幼儿的皮肤特点是表皮层较薄，平均厚度约为 40 μm[75]，而成年人的表皮层平均厚度约为 100 μm[76]。黄乃艳[77]对儿童、成人皮肤的表皮层厚度进行了数学仿真，发现在相同的 V-PDT 剂量下，儿童浅层血管的 $^1O_2$ 含量高于成人。Gan 等[73]用 V-PDT 治疗 82 名 1～14 岁的 PWS 患者，发现 1～2 岁的患者比 3～6 岁，7～14 岁的治疗效果好。Zhang 等[74]用 V-PDT 治疗婴儿面部 PWS 一次（平均年龄为 1.74 岁），随访有效率为 98%。而 Zhao 等[78]用 V-PDT 治疗青年和成人 PWS（14～65 岁）一次，随访有效率仅为 89.7%。除年龄外，同一个体的不同部位，表皮层厚度也有差异。Yu 等[79]取了 15 名病灶位于四肢的患者的病理，结果显示，肢体近端的角质层、表皮层的厚度均比中间、远端部位薄，同时 PDL 治疗的结果也显示，位于肢体近端的 PWS 的疗效优于病灶位于远端的。综上所述，对于具有较薄表皮层的婴幼儿和身体部位，在同样的光剂量下，到达病变血管的光子量较多，V-PDT 疗效较好。

4.3 血管管径

血管管径的粗细会显著影响光的穿透，从而影响光在组织的分布。Jacques[80]使用蒙特卡罗模型模拟了同一束光在不同粗细血管中的穿透，发现随着血管管径的增加，反射率增加，光不能覆盖整根血管。Tan 等[81]发现，在用波长为 577 nm 和 585 nm 的 PDL 治疗 PWS 时，血液对其的吸收系数分别为 430 cm^{-1} 和 200 cm^{-1}，穿透深度分别为 23 μm 和 50 μm，若血管管径大于 23 μm 和 50 μm，则血管中心和下部所吸收的能量十分有限，从而限制治疗效果。这一研究说明，血管管径的大小显著影响光的分布。

血管管径能表征 PWS 的病变程度，血管管径越大，病变颜色越深[26]。如表 2 所示，Waner 等[82]根据畸形血管的扩张程度，将 PWS 分为 I-V 级：I 级（血管管径为 50～80 μm）、II 级（血管管径为 80～100 μm）、III 级（血管管径为 100～120 μm）、IV 级（血管管径为 120～150 μm）和 V 级（血管管径在 150 μm 以上）。顾瑛等[19]根据皮色和皮肤是否增厚将 PWS 分为三（四）型：粉红（鲜红）、紫红和增厚型。该方法由于简单便捷，目前被广泛用于 PWS 的分型和术后疗效判断。黄乃艳等[71]用数学建模的方法模拟粉红、紫红、增厚型 PWS 的血管（血管管径分别为 60，120，180 μm）对 V-PDT 的响应，结果显示，管径粗的血管平均 $^1O_2$ 产量较管径细的血管少，管径粗的血管难以被破坏。可能原因是血管管径越粗，抵达血管中心和血管深层部分的光子数已经不足以激发光敏剂，血管内的 $^1O_2$ 产生不均匀，这种不均匀可能会导致管径较粗的血管的破坏不完全。Gan 等[73,83-84]在临床中同样发现，V-PDT 治疗粉红型的效果最佳，其次为紫红型，增厚型的疗效最差。除了病变类型外，同一个体不同部位的疗效也有差异。Yu 等[25]对 13 名病灶位于面部中心区和边缘区的患者进行活检，发现面部中心区、边缘区的血管平均管径分别为 46 μm 和 32 μm，平均深度为 510 μm 和 289 μm，进行 PDL 治疗后，中心区的褪色率不如边缘区。Han 等[85]用 V-PDT 治疗对 PDL 不敏感的 67 例 PWS 患者，发现 46.2%患者病灶显示出较好的褪色效果，同时发现中心区的治疗效果不如边缘区。

研究者通过使用无创光学技术也发现了以上规律。2014 年，Zhen 等[34]使用 OCT 检测了 43 名 PWS 病灶位于面部的患者（共 82 个检测部位）的血管管径和深度信息，将面部分为眶下区、耳前区、颧部和颞部。并对这 43 名患者进行 V-PDT 术后随访，观察血管管径与疗效之间的相关性，发现脸颊部的血管直径显著粗于其他三个面部区域，且 V-PDT 疗效最差，说明血管直径的增加会降低 V-PDT 疗效。2021 年，Ma 等[43]使用 PAI 观察了 5 名 PWS 患者 V-PDT 前后血管管径和深度的变化，发现术后平均血管管径变细、血管深度变浅的患者的 V-PDT 疗效更佳。2021 年，Fusano 等[86]采用 RCM 检测了 65 名 PWS 患者，总结了 PDL 难治型 PWS 的 RCM 表现为血管管径增粗，血管位置加深。

表 2 PWS 的临床分型

Table 2 Clinical classification of PWS

Ref.	Method	Classification	Characteristic
[88]	Histopathology	A: constricted type B: dilated type C: intermediate type D: deep located type	A: blood vessels are differed little from the normal pattern and their number is not more than that in normal skin B: vessels are considerably enlarged and often contain red cells C: this type shows histological features common to those of A and B types D: vessels scatter throughout dermis
[93]	Histopathology	Type I: dilated type Type II: dilated type with cavernous vascular malformation Type III: functional developmental type Type IV: cobblestone	Type I: number of vessels increase or blood vessels dilate, and surrounding tissues are normal Type II: this type shows dilated vessels with cavernous vascular malformation Type III: this type shows formation of single or multiple nodules Type IV: dilatation of blood vessels is throughout lesion
[38]	Dermoscope	Type I: blobs Type II: rings Type III: containing I and II	Type I: this type shows superficial, tortuous, dilated end capillary loops Type II: this type shows dilated vessels in superficial horizontal vascular plexus Type III: this type contains I and II
[27]	Histopathology	Grade I Grade II Grade III Grade IV Grade V	Grade I: vessel diameter is 50–80 μm Grade II: vessel diameter is 80–100 μm Grade III: vessel diameter is 100–120 μm Grade IV: vessel diameter is 120–150 μm Grade V: vessel diameter is >150 μm
[19]	Naked eyes	1: pink (red) 2: purple 3: thickening (nodules)	1: ectatic vessels are mostly located in papillary layer (pink); ectatic vessels are mostly located in middle dermis layer (red) 2: dilated vessels are mostly located in papillary and middle dermis layers, however, some are located in deep dermis and presented like cluster 3: dilated vessels are distributed from superficial to deep dermis layers and even to subcutaneous tissue, presenting like cluster[94]

4.4 血管深度

血管在皮肤不同深浅位置的分布也会显著影响光在组织的分布，进而影响 V-PDT 疗效。理论上，对于单根血管，由于皮肤对光的吸收和散射，其位置越深，吸收的能量越少。实际上，PWS 的血管分布很复杂，是多层排列的柱状血管，它们会对激光的分布有一定影响。通过数学仿真得出，如果深层有血管，浅层血管吸收的光能量会减少，这是因为深层血管对光的吸收使散射到浅层血管的光减少。如果层与层之间的距离加大，则浅层血管吸收的光能量增多，而深层血管吸收的能量减少。如果行与行之间的距离加大，每一层血管吸收的光能量都会增加，因为从间隔组织中散射到每一层血管的光都会有所增加[77]。此外，如果深层血管的表面还有血管，深层血管吸收的光能会减少。因此，若要使深层血管吸收光的能量达到破坏量，必须是浅层血管已经被破坏，这就是用 V-PDT 治疗 PWS 通常需要几个疗程的原因。

以上仅是理论知识和数学模型得出的推论，由于目前金标准病理活检采集的组织仅能提供一个断面的信息，无法综合考量整体病灶血管位置分布对 V-PDT 的影响。但仍有学者探索了血管的平均深度对治疗的影响。如前所述，面部中心区的血管位置比边缘区深，故治疗效果下降。除面部外，肢体的不同部位，血管深度也不一致。Yu 等[79]在治疗前取上肢近端、中部和远端的病理活检，发现近端的平均血管深度比中间、远端部位更加浅。对于不同病变类型的患者，病变血管的位置分布同样深浅不一。苑凯华[24]从 11 名红型、14 名紫型、7 名增厚型 PWS 患者病灶区取了 32 块病理组织，分析后得出红型、紫型、增厚型患者的平均血管深度分别为(0.42±0.07)mm、(0.54±0.07)mm、(0.65±0.08)mm。说明随着病情的加重，血管平均位置加深。如前所述，Gan 等[73,83-84]发现，V-PDT 治疗粉红型的效果最佳，其次为紫红型，增厚型的疗效最差，故也显示了血管位置越深，治疗效果越差。

4.5 血管形态

PWS 病理结构是由真皮乳头层和网状层内发育畸形、扩张的毛细血管组成。扩张的血管不规则，有垂直于皮肤表面的，也有弯曲成弧线的。有学者数学仿

真了这两种血管模型，发现对于垂直于皮肤表面的柱状血管，只有靠近表面的部分能吸收较多的光能。对于弧线形的血管，弯向皮肤表面的部分吸收了较多的光能，而伸向真皮深层的两脚则吸收的能量较少，这说明对于形状复杂的血管，其破坏可能是呈节段状，不能一次完全均匀地消失[77]。在 PWS 空间形态的获取上，Smithies 等[87]在一个对 PDL 无反应的患处取了病理组织，该病灶位于前臂，呈浅紫色，对其进行连续切片、HE 染色后再进行三维重构，发现该处由多个小管径（10～50 μm）的血管簇组成，说明小血管、高度簇集、复杂形态的血管团可能会限制疗效。

此外，如表 2 所示，国外学者尝试按病理特点及皮肤镜特点与 PDL 疗效之间的关系对 PWS 进行分型。1981 年，Ohmori 等[88]收集了 1264 例 PWS 患者的 1348 个病理标本，将其分为收缩型、扩张型、中间型和深部型四型，发现扩张型的 PDL 治疗效果最好，其次为中间型和收缩型，深部型的效果最差。1984 年，Finley 等[89]分析了 500 例 PWS 病理标本后又提出了四型病理分型法：Ⅰ型为扩张型，Ⅱ型为扩张伴海绵状血管畸形，Ⅲ型为功能发展型，Ⅳ型为卵石型，同样发现扩张型的疗效最佳。不过尚未有大样本病理标本形态与 V-PDT 疗效相关性的相关研究，由于 PWS 病灶多位于面部，活检病人难以接受，未来可通过无创光诊断设备进行相关研究。根据皮肤镜下 PWS 血管形态特点与 PDL 疗效的相关性建立的 PWS 临床分型见 3.4 节。2019 年，Wen 等[90]使用皮肤镜观察 V-PDT 前后 22 名 PWS 患者血管的形态，发现粉红型表现为Ⅰ型（亮红的背景），病变深度浅；紫型表现为Ⅱ型（深红色的背景），病变深度加深；增厚型患者的血管呈团块样（暗红色的背景）。皮肤镜观察到出现血管破裂现象的 V-PDT 疗效更佳，研究者提出这一现象可以作为 V-PDT 治疗的终点。但目前皮肤镜观察的血管形态与 V-PDT 疗效的关系研究较少，仍需更多的研究。

以上研究均说明血管形态与 V-PDT 疗效之间具有相关性，但目前相关研究仍局限在病理活检上，而病理活检的结果是二维的，较难完全表征出血管形态与疗效之间的关系，OCTA/ODT、PAI 均可三维重构血管结构，其探测出的形态与疗效之间的关系将是未来研究的发展方向。

4.6 血流灌注

除了结构信息外，也有 V-PDT 治疗前后血流灌注量的变化与 V-PDT 疗效的关系的相关研究。LDI 和 LSI 均可对 PWS 进行功能成像并获取 PWS 区域的血流灌注信息[52,70]。1998 年，Jiang 等[50]采用 LDI 检测了 28 个 PWS 病灶区在 V-PDT 治疗前后的血流灌注量变化，发现所有病灶的血流灌注量在治疗后均发生下降，而且灌注量改变与 V-PDT 疗效呈现较好的相关性，显示了 LDI 用于 V-PDT 疗效评估的潜力。2014 年，Chen 等[91]使用 LDI 研究了 V-PDT 治疗前和治疗过程中 PWS 血流灌注量的变化，发现术前病灶区的灌注量高于或等于对侧正常区，术中 PWS 的血流灌注量呈现出先上升后缓慢下降的变化趋势。2014 年，Ren 等[92]使用 LSI 检测 V-PDT 治疗 PWS 前后血流灌注量的情况，发现术后 3～6 个月内血流灌注量显著下降的患者疗效更好，表明 LSI 检测结果与病变颜色消退呈现较好的相关性，显示了 LSI 可以评估 V-PDT 治疗 PWS 的疗效。以上研究均说明，V-PDT 前后血流灌注量的下降越多，治疗的效果越好。

4.7 小 结

本节总结了目前常见的 PWS 病灶结构（黑色素含量、表皮层厚度、血管深度、血管形态以及血流灌注量）对 V-PDT 疗效的影响以及目前可用于获取这些信息的主流无创光学成像方法。如表3所示，PAI可

表 3 PWS 病灶结构与 V-PDT 疗效的关系

Table 3 Relationship between PWS lesion structure and V-PDT efficacy

Factor	Optical method	Relationship	Reason
Melanin	PAI	(－)	It is located in epidermis, influencing optical absorbance
Epidermis thickness	PAI OCT	(－)	It varies for different individuals and parts of body and influences light penetration depth
Vascular diameter	PAI OCT/ODT/OCTA RCM	(－)	The larger the vessels, the less light can reach and cover entire vessel
Vascular depth	PAI OCT/ODT/OCTA RCM	(－)	The deeper vessels are, the less energy of light that vessels can absorb
Vascular morphology	PAI OCT/ODT/OCTA Dermoscope	Perpendicular (－)	Perpendicular vessels absorb less light than curved ones
Blood perfusion	LDI LSI	Decreased after V-PDT (＋)	Decreased blood perfusion is equal to decreased number of dilated vessels

Note: (－), negative effect; (＋), positive effect

以获取黑色素含量和表皮层厚度，OCT 可以获取表皮层厚度，表皮层黑色素含量越多，表皮层厚度越厚，则黑色素和表皮层对光的吸收和阻挡作用越强，到达病变血管的光子量越少，V-PDT 疗效越差；PAI、OCT/ODT/OCTA、RCM 可以获取血管管径和血管深度，血管越粗，位置越深，V-PDT 疗效越差；PAI、OCT/ODT/OCTA、皮肤镜可以获取血管形态，其与 V-PDT 疗效之间具有相关性，如垂直血管的比例越高，由于仅有靠近表面的部分血管吸收较多的光能，故 V-PDT 疗效越差；利用激光多普勒成像和激光散斑可以获取血流灌注量，通过探测 V-PDT 治疗前后 PWS 病灶区血流灌注量的变化，发现治疗后血流灌注量的下降越多，V-PDT 疗效较好。

5 结束语

尽管 V-PDT 已成为国内治疗 PWS 的一线方案，但 V-PDT 精准诊疗的瓶颈是 PWS 病灶结构的缺失。随着无创光学诊断设备的不断发展和优化及其在 PWS 临床应用研究中的不断深入，可通过获取 PWS 病灶结构来进行术前诊断分级以及术后疗效的精准评估，并通过观察 V-PDT 治疗过程中 PWS 病灶结构的改变来进行术中方案优化，进而为 V-PDT 方案的个性化和精准化制定提供重要支持。

参 考 文 献

[1] Techasatian L, Sanaphay V, Paopongsawan P, et al. Neonatal birthmarks: a prospective survey in 1000 neonates[J]. Global Pediatric Health, 2019, 6: 1-8.

[2] Rivers J K, Frederiksen P C, Dibdin C. A prevalence survey of dermatoses in the Australian neonate [J]. Journal of the American Academy of Dermatology, 1990, 23(1): 77-81.

[3] Jacobs A H, Walton R G. The incidence of birthmarks in the neonate[J]. Pediatrics, 1976, 58(2): 218-222.

[4] Smoller B R, Rosen S. Port-wine stains. A disease of altered neural modulation of blood vessels?[J]. Archives of Dermatology, 1986, 122(2): 177-179.

[5] Shafirstein G, Bäumler W, Lapidoth M, et al. A new mathematical approach to the diffusion approximation theory for selective photothermolysis modeling and its implication in laser treatment of port-wine stains [J]. Lasers in Surgery and Medicine, 2004, 34(4): 335-347.

[6] Fiskerstrand E J, Svaasand L O, Kopstad G, et al. Photothermally induced vessel-wall necrosis after pulsed dye laser treatment: lack of response in port-wine stains with small sized or deeply located vessels [J]. Journal of Investigative Dermatology, 1996, 107(5): 671-675.

[7] Klein A, Bäumler W, Landthaler M, et al. Laser and IPL treatment of port-wine stains: therapy options, limitations, and practical aspects[J]. Lasers in Medical Science, 2011, 26(6): 845-859.

[8] Geronemus R G, Ashinoff R. The medical necessity of evaluation and treatment of port-wine stains[J]. The Journal of Dermatologic Surgery and Oncology, 1991, 17(1): 76-79.

[9] Troilius A, Wrangsjö B, Ljunggren B. Patients with port-wine stains and their psychosocial reactions after photothermolytic treatment[J]. Dermatologic Surgery: Official Publication for American Society for Dermatologic Surger, 2000, 26(3): 190-196.

[10] Babilas P, Schreml S, Eames T, et al. Split-face comparison of intense pulsed light with short- and long-pulsed dye lasers for the treatment of port-wine stains [J]. Lasers in Surgery and Medicine, 2010, 42(8): 720-727.

[11] Anderson R R, Parrish J A. Selective photothermolysis: precise microsurgery by selective absorption of pulsed radiation [J]. Science, 1983, 220(4596): 524-527.

[12] Savas J A, Ledon J A, Franca K, et al. Pulsed dye laser-resistant port-wine stains: mechanisms of resistance and implications for treatment[J]. The British Journal of Dermatology, 2013, 168(5): 941-953.

[13] Phung T L, Oble D A, Jia W C, et al. Can the wound healing response of human skin be modulated after laser treatment and the effects of exposure extended? Implications on the combined use of the pulsed dye laser and a topical angiogenesis inhibitor for treatment of port wine stain birthmarks[J]. Lasers in Surgery and Medicine, 2008, 40(1): 1-5.

[14] Marqués L, Núñez-Córdoba J M, Aguado L, et al. Topical rapamycin combined with pulsed dye laser in the treatment of capillary vascular malformations in Sturge-Weber syndrome: phase II, randomized, double-blind, intraindividual placebo-controlled clinical trial[J]. Journal of the American Academy of Dermatology, 2015, 72(1): 151-158.

[15] Katugampola G A, Lanigan S W. Five years' experience of treating port wine stains with the flashlamp-pumped pulsed dye laser[J]. The British Journal of Dermatology, 1997, 137(5): 750-754.

[16] Jia W C, Sun V, Tran N, et al. Long-term blood vessel removal with combined laser and topical rapamycin antiangiogenic therapy: implications for effective port wine stain treatment[J]. Lasers in Surgery and Medicine, 2010, 42(2): 105-112.

[17] Huikeshoven M, Koster P H L, de Borgie C A J M, et al. Redarkening of port-wine stains 10 years after pulsed-dye-laser treatment[J]. The New England Journal of Medicine, 2007, 356(12): 1235-1240.

[18] Gu Y, Huang N Y, Liang J, et al. Clinical study of 1949 cases of port wine stains treated with vascular photodynamic therapy (Gu's PDT)[J]. Annales De Dermatologie et De Venereologie, 2007, 134(3): 241-244.

[19] 顾瑛，李峻亨，江亿平，等. 光动力学疗法选择性治疗鲜红斑痣的临床研究附 40 例报告[J]. 中国激光医学杂志，1992，1(1)：16-20.
Gu Y, Li J H, Jiang Y P, et al. A clinical study of photodynamic therapy for port wine stain-a report of 40 cases [J]. Chinese Journal of Laser Medicine & Surgery, 1992, 1(1): 6-10.

[20] 顾瑛，李峻亨，单焕炎，等. 铜蒸汽激光用于光动力疗法治疗鲜红斑痣 50 例疗效分析[J]. 中国激光医学杂志，1994，3(4)：215-217.
Gu Y, Li J H, Shan H Y, et al. Clinical application of copper vapor laser in PDT for fifty cases of PWS[J]. Chinese Journal of Laser Medicine & Surgery, 1994, 3(4): 215-217.

[21] Qin Z P, Li K L, Ren L, et al. Photodynamic therapy of port wine stains—a report of 238 cases [J]. Photodiagnosis and Photodynamic Therapy, 2007, 4(1): 53-59.

[22] Qiu H X, Gu Y, Wang Y, et al. Twenty years of clinical experience with a new modality of vascular-targeted photodynamic therapy for port wine stains [J]. Dermatologic Surgery: Official Publication for American Society for Dermatologic Surgery, 2011, 37(11): 1603-1610.

[23] Gao K, Huang Z, Yuan K H, et al. Side-by-side comparison of photodynamic therapy and pulsed-dye laser treatment of port-wine stain birthmarks[J]. The British Journal of Dermatology, 2013, 168(5): 1040-1046.

[24] 苑凯华. 鲜红斑痣畸形血管结构的光学检测及与疗效关系的研究[D]. 广州：南方医科大学，2012：62-81.
Yuan K H. Optical detection the structure of malformed vessels in port wine stain and research of the relationship with treatment

efficacy[D]. Guangzhou: Southern Medical University, 2012: 62-81.

[25] Yu W X, Ma G, Qiu Y J, et al. Why do port-wine stains (PWS) on the lateral face respond better to pulsed dye laser (PDL) than those located on the central face?[J]. Journal of the American Academy of Dermatology, 2016, 74(3): 527-535.

[26] Elibieta H P, Kurzyna A. Hemangiomas and vascular malformations of the head and neck[J]. Otolaryngologia Polska, 2006, 60(5): 663-674.

[27] 周国瑜, 张志愿, 李江. 52 例鲜红斑痣颜色类别的病理图像计算机分析[J]. 口腔颌面外科杂志, 1999, 9(2): 112-115.
Zhou G Y, Zhang Z Y, Li J. Computed assessment of pathological images on 52 case' biopsies of port wine stain[J]. Journal of Oral and Maxillofacial Surgery, 1999, 9(2): 112-115.

[28] 刘凡光, 顾瑛, 于常青, 等. 光敏剂漂白特性在鲜红斑痣光动力治疗中的作用[J]. 中国激光医学杂志, 2002, 11(3): 137-140.
Liu F G, Gu Y, Yu C Q, et al. Effect of photosensitizer photobleaching on vascular selectivity of photodynamic therapy [J]. Chinese Journal of Laser Medicine & Surgery, 2002, 11(3): 137-140.

[29] 顾瑛, 李峻亨, 江亿平, 等. 光动力疗法选择性治疗鲜红斑痣的机制探讨[J]. 中国激光医学杂志, 1992(3): 141-144, 177.
Gu Y, Li J H, Jiang Y P, et al. A study on the mechanism of photodynamic therapy for port wine stains[J]. Cinese Journal of Laser Medicine & Surgery, 1992(3): 141-144, 177.

[30] 李文博, 沈毅, 李步洪. 光学成像技术在光动力剂量监测中的应用进展[J]. 中国激光, 2020, 47(2): 0207006.
Li W B, Shen Y, Li B H. Advances in optical imaging for monitoring photodynamic therapy dosimetry [J]. Chinese Journal of Lasers, 2020, 47(2): 0207006.

[31] Chen B, Pogue B W, Hoopes P J, et al. Vascular and cellular targeting for photodynamic therapy [J]. Critical Reviews in Eukaryotic Gene Expression, 2006, 16(4): 279-305.

[32] Zhao S Y, Gu Y, Xue P, et al. Imaging port wine stains by fiber optical coherence tomography [J]. Journal of Biomedical Optics, 2010, 15(3): 036020.

[33] Zhou Y, Yin D Q, Xue P, et al. Imaging of skin microvessels with optical coherence tomography: potential uses in port wine stains[J]. Experimental and Therapeutic Medicine, 2012, 4(6): 1017-1021.

[34] Zhen J, Wang C M, Wang Y, et al. Optical coherence tomography: a potential tool for prediction of treatment response for port wine stain after photodynamic therapy [J]. Proceedings of SPIE, 2014, 9268: 926807.

[35] 王成铭. OCT 超高速成像方法研究及在临床和法庭科学中的应用[D]. 北京: 清华大学, 2018: 39-53.
Wang C. Ultrahigh speed OCT and its applications in clinical and forensic study[D]. Beijing: Tsinghua University, 2018: 39-53.

[36] Astner S, González S, Cuevas J, et al. Preliminary evaluation of benign vascular lesions using *in vivo* reflectance confocal microscopy[J]. Dermatologic Surgery: Official Publication for American Society for Dermatologic Surgery, 2010, 36(7): 1099-1110.

[37] Ren J, Qian H, Xiang L H, et al. The assessment of pulsed dye laser treatment of port-wine stains with reflectance confocal microscopy[J]. Journal of Cosmetic and Laser Therapy, 2014, 16(1): 21-25.

[38] Motley R J, Lanigan S W, Katugampola G A. Videomicroscopy predicts outcome in treatment of port-wine stains[J]. Archives of Dermatology, 1997, 133(7): 921-922.

[39] Sevila A, Nagore E, Botella-Estrada R, et al. Videomicroscopy of venular malformations (port-wine stain type): prediction of response to pulsed dye laser[J]. Pediatric Dermatology, 2004, 21(5): 589-596.

[40] Viator J A, Au G, Paltauf G, et al. Clinical testing of a photoacoustic probe for port wine stain depth determination[J]. Lasers in Surgery and Medicine, 2002, 30(2): 141-148.

[41] Viator J A, Choi B, Ambrose M, et al. *In vivo* port-wine stain depth determination with a photoacoustic probe [J]. Applied Optics, 2003, 42(16): 3215-3224.

[42] Kolkman R G M, Mulder M J, Glade C P, et al. Photoacoustic imaging of port-wine stains[J]. Lasers in Surgery and Medicine, 2008, 40(3): 178-182.

[43] Ma H G, Cheng Z W, Wang Z Y, et al. Quantitative and anatomical imaging of dermal angiopathy by noninvasive photoacoustic microscopic biopsy[J]. Biomedical Optics Express, 2021, 12(10): 6300-6316.

[44] Wang Z, Yang F, Ma H, et al. Bifocal 532/1064 nm alternately illuminated photoacoustic microscopy for capturing deep vascular morphology in human skin [J]. Journal of the European Academy of Dermatology and Venereology: JEADV, 2022, 36(1): 51-59.

[45] Latrive A, Teixeira L R, Gomes A S, et al. Characterization of skin Port-Wine Stain and Hemangioma vascular lesions using Doppler OCT[J]. Skin Research and Technology, 2016, 22(2): 223-229.

[46] Waibel J S, Holmes J, Rudnick A, et al. Angiographic optical coherence tomography imaging of hemangiomas and port wine birthmarks[J]. Lasers in Surgery and Medicine, 2018: 1-9.

[47] Liu Y D, Zhu D, Xu J J, et al. Penetration-enhanced optical coherence tomography angiography with optical clearing agent for clinical evaluation of human skin [J]. Photodiagnosis and Photodynamic Therapy, 2020, 30: 101734.

[48] Mehrabi J N, Holmes J, Abrouk M, et al. Vascular characteristics of port wine birthmarks as measured by dynamic optical coherence tomography [J]. Journal of the American Academy of Dermatology, 2021, 85(6): 1537-1543.

[49] Troilius A M, Ljunggren B. Evaluation of port wine stains by laser Doppler perfusion imaging and reflectance photometry before and after pulsed dye laser treatment[J]. Acta Dermato-Venereologica, 1996, 76(4): 291-294.

[50] Jiang L, Gu Y, Li X, et al. Changes of skin perfusion after photodynamic therapy for port wine stain[J]. Chinese Medical Journal, 1998, 111(2): 136-138.

[51] Mermod T, El Ezzi O, Raffoul W, et al. Assessment of the role of LASER-Doppler in the treatment of port-wine stains in infants [J]. Journal of Pediatric Surgery, 2015, 50(8): 1388-1392.

[52] Chen D F, Ren J, Wang Y, et al. Intraoperative monitoring of blood perfusion in port wine stains by laser Doppler imaging during vascular targeted photodynamic therapy: a preliminary study[J]. Photodiagnosis and Photodynamic Therapy, 2016, 14: 142-151.

[53] Huang Y C, Tran N, Shumaker P R, et al. Blood flow dynamics after laser therapy of port wine stain birthmarks[J]. Lasers in Surgery and Medicine, 2009, 41(8): 563-571.

[54] Yang B, Yang O, Guzman J, et al. Intraoperative, real-time monitoring of blood flow dynamics associated with laser surgery of port wine stain birthmarks [J]. Lasers in Surgery and Medicine, 2015, 47(6): 469-475.

[55] Xue P. Development of high-performance optical coherence tomography[J]. Chinese Journal of Lasers-Zhongguo Jiguang, 2021, 48(15): 398-408.

[56] Barton J, Welch A, Izatt J. Investigating pulsed dye laser-blood vessel interaction with color Doppler optical coherence tomography[J]. Optics Express, 1998, 3(6): 251-256.

[57] Li Y, Wei W, Wang R K. Capillary flow homogenization during functional activation revealed by optical coherence tomography angiography based capillary velocimetry[J]. Scientific Reports, 2018, 8: 4107.

[58] Zhao Y, Brecke K M, Ren H, et al. Three-dimensional reconstruction of *in vivo* blood vessels in human skin using phase-resolved optical Doppler tomography[J]. IEEE Journal of Selected Topics in Quantum Electronics, 2001, 7(6): 931-935.

[59] Barsky S H, Rosen S, Geer D E, et al. The nature and evolution of port wine stains: a computer-assisted study [J].

Journal of Investigative Dermatology, 1980, 74(3): 154-157.
[60] Pattyn A, Mumm Z, Alijabbari N, et al. Model-based optical and acoustical compensation for photoacoustic tomography of heterogeneous mediums[J]. Photoacoustics, 2021, 23: 100275.
[61] 龙晓云, 田超. 生物医学光声显微成像: 技术和应用进展[J]. 中国激光, 2020, 47(2): 0207016.
Long X Y, Tian C. Biomedical photoacoustic microscopy: advances in technology and applications[J]. Chinese Journal of Lasers, 2020, 47(2): 0207016.
[62] Shahriari N, Grant-Kels J M, Rabinovitz H, et al. Reflectance confocal microscopy: diagnostic criteria of common benign and malignant neoplasms, dermoscopic and histopathologic correlates of key confocal criteria, and diagnostic algorithms[J]. Journal of the American Academy of Dermatology, 2021, 84(1): 17-31.
[63] Rajadhyaksha M, González S, Zavislan J M, et al. *In vivo* confocal scanning laser microscopy of human skin II: advances in instrumentation and comparison with histology[J]. Journal of Investigative Dermatology, 1999, 113(3): 293-303.
[64] Rajadhyaksha M, Grossman M, Esterowitz D, et al. *In vivo* confocal scanning laser microscopy of human skin: melanin provides strong contrast[J]. Journal of Investigative Dermatology, 1995, 104(6): 946-952.
[65] Sharif S A, Taydas E, Mazhar A, et al. Noninvasive clinical assessment of port-wine stain birthmarks using current and future optical imaging technology: a review[J]. The British Journal of Dermatology, 2012, 167(6): 1215-1223.
[66] Chang C J, Yu J S, Nelson J S. Confocal microscopy study of neurovascular distribution in facial port wine stains (capillary malformation)[J]. Journal of the Formosan Medical Association, 2008, 107(7): 559-566.
[67] Marghoob N, Navarrete-Dechent C, Liopyris K, et al. Dermoscopic features of benign vascular lesions presenting on volar skin: a case series and literature review[J]. Journal of the European Academy of Dermatology and Venereology, 2019, 33(12): 444-445.
[68] Eubanks L E, McBurney E I. Videomicroscopy of port-wine stains: correlation of location and depth of lesion[J]. Journal of the American Academy of Dermatology, 2001, 44(6): 948-951.
[69] Basak K, Manjunatha M, Dutta P K. Review of laser speckle-based analysis in medical imaging[J]. Medical & Biological Engineering & Computing, 2012, 50(6): 547-558.
[70] Chen D F, Ren J, Wang Y, et al. Relationship between the blood perfusion values determined by laser speckle imaging and laser Doppler imaging in normal skin and port wine stains[J]. Photodiagnosis and Photodynamic Therapy, 2016, 13: 1-9.
[71] 黄乃艳, 顾瑛, 刘凡光, 等. 光动力学治疗鲜红斑痣反应体系数学仿真的初步探讨[J]. 中国激光医学杂志, 2005, 14(2): 83-89.
Huang N Y, Gu Y, Liu F G, et al. Preliminary exploration of mathematical simulation of photodynamic treatment on port wine stains' reaction system[J]. Chinese Journal of Laser Medicine & Surgery, 2005, 14(2): 83-89.
[72] Garden J M. Laser removal of port wine stains: how close are we? Acommentary[J]. Lasers in Surgery and Medicine, 2007, 39(7): 569-570.
[73] Gan L Q, Wang H, Ni S L, et al. A clinical study of HMME-PDT therapy in Chinese pediatric patients with port-wine stain[J]. Photodiagnosis and Photodynamic Therapy, 2018, 23: 102-105.
[74] Zhang Y J, Yang Y G, Zhang Z, et al. Clinical study on hemoporfin PDT for infant facial port-wine stains[J]. Photodiagnosis and Photodynamic Therapy, 2019, 25: 106-110.
[75] Wang D, Fu H. Histological map of human skin (color)[M]. Jinan: Shandong Science and Technology Press, 1999.
[76] Savchenko E P, Tuchin V V. Monte Carlo simulation of light propagation in multilayered tissue with cleared inclusions[J]. Proceedings of SPIE, 2001, 4432: 247-252.
[77] 黄乃艳. 光动力疗法治疗鲜红斑痣的数学模型的建立及验证[D]. 北京: 中国人民解放军医学院, 2005: 114-115.
Huang N Y. Mathematical modeling and verification study on photodynamic therapy for port wine stains[D]. Beijing: Chinese PLA Medical School, 2005: 114-115.
[78] Zhao Y, Tu P, Zhou G Y, et al. Hemoporfin photodynamic therapy for port-wine stain: a randomized controlled trial[J]. PLoS One, 2016, 11(5): e0156219.
[79] Yu W X, Zhu J F, Han Y, et al. Assessment of outcomes with pulsed dye laser treatment of port-wine stains located proximally vs distally on extremities[J]. JAMA Dermatology, 2020, 156(6): 702-704.
[80] Jacques S L. Optical assessment of cutaneous blood volume depends on the vessel size distribution: a computer simulation study[J]. Journal of Biophotonics, 2010, 3(1/2): 75-81.
[81] Tan O T, Morrison P, Kurban A K. 585 nm for the treatment of port-wine stains[J]. Plastic and Reconstructive Surgery, 1990, 86(6): 1112-1117.
[82] Waner M, Suen J Y. Hemangiomas and vascular malformations of the head and neck[M]. Singapore: John Wiley & Sons Inc; 1999.
[83] 顾瑛, 刘凡光, 王开, 等. 光动力疗法治疗鲜红斑痣 1216 例临床分析[J]. 中国激光医学杂志, 2001, 10(2): 86-89.
Gu Y, Liu F G, Wang K, et al. A clinic analysis of 1216 cases of port wine stain treated by photodynamic therapy[J]. Chinese Journal of Laser Medicine & Surgery, 2001, 10(2): 86-89.
[84] Li D C, Nong X, Hu Z Y, et al. Efficacy and related factors analysis in HMME-PDT in the treatment of port wine stains[J]. Photodiagnosis and Photodynamic Therapy, 2020, 29: 101649.
[85] Han Y, Ying H R, Zhang X L, et al. Retrospective study of photodynamic therapy for pulsed dye laser-resistant port-wine stains[J]. The Journal of Dermatology, 2020, 47(4): 348-355.
[86] Fusano M, Bencini P L. Capillaroscopy and reflectance confocal microscopy characterization of refractory port-wine stains[J]. Lasers in Medical Science, 2021, 36(2): 407-412.
[87] Smithies D J, van Gemert M J, Hansen M K, et al. Three-dimensional reconstruction of port wine stain vascular anatomy from serial histological sections[J]. Physics in Medicine and Biology, 1997, 42(9): 1843-1847.
[88] Ohmori S, Huang C K. Recent progress in the treatment of portwine staining by argon laser: some observations on the prognostic value of relativespectro-reflectance (RSR) and the histological classification of the lesions[J]. British Journal of Plastic Surgery, 1981, 34(3): 249-257.
[89] Finley J L, Noe J M, Arndt K A, et al. Port-wine stains. Morphologic variations and developmental lesions[J]. Archives of Dermatology, 1984, 120(11): 1453-1455.
[90] Wen L, Zhang Y F, Zhang L L, et al. Application of different noninvasive diagnostic techniques used in HMME-PDT in the treatment of port wine stains[J]. Photodiagnosis and Photodynamic Therapy, 2019, 25: 369-375.
[91] Chen D F, Ren J, Wang Y, et al. Laser Doppler line scanner for monitoring skin perfusion changes of port wine stains during vascular-targeted photodynamic therapy[J]. Proceedings of SPIE, 2014: 9268-92681.
[92] Ren J, Li P C, Zhao H Y, et al. Assessment of tissue perfusion changes in port wine stains after vascular targeted photodynamic therapy: a short-term follow-up study[J]. Lasers in Medical Science, 2014, 29(2): 781-788.
[93] Finley J L, Clark R A, Colvin R B, et al. Immunofluorescent staining with antibodies to factor VIII, fibronectin, and collagenous basement membrane protein in normal human skin and port wine stains[J]. Archives of Dermatology, 1982, 118(12): 971-975.
[94] 李勤. 鲜红斑痣激光疗效测评方法的建立及临床应用研究[D]. 广州: 南方医科大学, 2007: 31-32.
Li Q. Establish of assessment system for curative effects of laser

treatment on nevus flammeus and its clinical application[D]. Guangzhou: Southern Medical University, 2007: 31-32.

Progress in Port-Wine Stains Lesion Structure and Its Optical Imaging Technique in Vascular-Targeted Photodynamic Therapy

Liu Yidi[1,2], Chen Defu[3], Zeng Jing[2], Qiu Haixia[2**], Gu Ying[2,3,4*]

[1] *Medical School of Chinese PLA, Beijing* 100853, *China*;

[2] *Department of Laser Medicine, the First Medical Center, Chinese PLA General Hospital, Beijing* 100853, *China*;

[3] *School of Medical Technology, Beijing Institute of Technology, Beijing* 100081, *China*;

[4] *Precision Laser Medical Diagnosis and Treatment Innovation Unit, Chinese Academy of Medical Sciences, Beijing* 100730, *China*

Abstract

Significance Port wine stain (PWS), a skin disease with an incidence of 0.3%–0.5% in infants, is attributed to congenital and progressive cutaneous vascular malformations. PWS lesions appear as purplish red or pink patches on skin. PWS commonly occurs on the face and neck, but it can also appear anywhere on the body (e.g., arms or legs). PWS lesions give patients an extremely severe psychological burden about their cosmetic appearance, which may greatly reduce their life quality. The majority of PWS lesions darkens in color and thickens as time goes by. PWS lesions can become aggravated, leading to progressive disfigurement. Thus, early intervention and treatments are urgent to reduce the likelihood and severity of disfigurement and psychosocial morbidity.

The key point of treating PWS is to selectively and precisely destroy the abnormal blood vessels that cause the discolored lesions. Vascular-targeted photodynamic therapy (V-PDT) has been introduced and remarked as the golden standard of the therapy for PWS in China since the early 1990s, which destroys the ectatic vessesls by using the double selectivity of light and photosensitizer. Several clinical studies show that V-PDT is safe and effective in the treatment of PWS at all ages. Nevertheless, there are still some patients who have relatively low sensitivity to V-PDT. The unsatisfied therapeutic outcome may result from the heterogeneity and complexity of the PWS morphological parameters. Therefore, mastering the relationship between PWS lesion structure and V-PDT efficacy is beneficial to the development of therapeutic plan and the assessment of prognosis.

Skin biopsy is considered as the golden standard of acquiring the information of PWS lesion structure. Nevertheless, it is invasive which may lead to hypersensitivity to local anaesthetic agents, pain of local anaesthesia, bleeding, infection, and scarring. Hence, a painless and non-invasive imaging method for the *in vivo* assessment of PWS lesion structure will greatly benefit V-PDT treatments. With the development of optical imaging techniques, nowadays, they have showed much potential in obtaining the information of histopathology. Here, the relationship between PWS lesion structure (epidermis thickness, vascular diameter and depth, etc.) and V-PDT efficacy is summarized. In addition, the development of optical imaging techniques for obtaining PWS lesion structure is also reported.

Progress Optical coherence tomography (OCT) called 'optical biopsy' has been greatly developed in recent 20 years. Conventional OCT is used to visualize the fine structures of skin tissue although it is not an ideal tool for visualizing cutaneous vessels. As a functional modality of OCT, optical Doppler tomography (ODT) and optical coherence tomography angiography (OCTA) with the use of conjunction with sophistic algorism can provide a powerful tool to visualize and quantitatively analyze the cutaneous vascular networks. ODT and OCTA enhance the blood flow contrast by extracting moving particles (red blood cells) from static tissues without dye injection. To sum up, OCT/ODT/OCTA are capable of acquiring the epidermis thickness, the diameter and depth of vessels. Moreover, ODT/OCTA can further image a three-dimensional (3D) vascular system. However, OCT/ODT/OCTA have a relatively shallow imaging depth (less than 1 mm) because it is based on the optical imaging mechanism.

Photoacoustic imaging (PAI) combines the optical and ultrasonic merits is used to reduce the tissue scattering of photons with one-way ultrasound detection, while retaining the high optical contrast. Moreover, it can image over a 1 mm depth in skin. As an optical-contrast-based imaging technique, the photoacoustic imaging detects the endogenous skin chromophores, i.e., melanin and haemoglobin. PAI can obtain the content of melanin in epidermis, epidermis thickness, and vascular diameter and depth. Moreover, it can also achieve a 3D image of PWS vessels. However, PAI is a contact technique, in which a coupling medium (such as water and ultrasound gel) is required between the detector and tissue surface. Thus, it is unsuitable for an intraoperative use.

Reflectanceconfocal microscopy (RCM) is also a commonly used clinical skin diagnostic device. It uses a low-intensity near-infrared laser to first scan the skin horizontally, and then collects the backscattered light for imaging. RCM is the

relatively mature imaging equipment and it can obtain the depth and diameter of skin vessels, nevertheless, it has the drawbacks of two-dimensional (2D) imaging and shallow imaging depth (200–350 μm).

Dermoscope is an imaging device that can magnify tens or even hundreds of times and eliminate the reflected light on the skin surface. Skin pigment and blood vessels are the two main elements of its observation, which have been widely used in the clinical practice. Although the dermoscope is convenient to use and fast to image, its imaging depth is limited (~250 μm), which cannot completely reflect the overall structure of PWS lesions, and the PWS manifestations under the dermoscope are irregular. Currently, the clinical application of dermoscope in PWS is still few.

Laser Doppler imaging (LDI) and laser speckle imaging (LSI) are able to get the information of blood perfusion, however, they only offer 2D information and the resolution is relatively low.

By applying the above techniques to obtain PWS lesion structure or biopsy, the relationship between PWS lesion structure and V-PDT efficacy is obtained as follows. In terms of melanin content in epidermis, it has the negative effect towards the V-PDT efficacy. It locates at the epidermis, absorbs the light, and influences optical absorbance. As for the epidermis thickness, it varies for different individuals and parts of the body, and affects the light penetration depth. Hence, it also has the negative effects towards V-PDT efficacy. In terms of vessels diameter, the larger the vessels, the less light can reach and cover the entire vessel. As for the vascular depth, the deeper the vessels are, the less light energy the vessels can absorb. The vascular morphological parameters also influence the efficacy. If the ratio of perpendicular vessels is higher than that of the curved ones, the efficacy is reduced due to the fact that the perpendicular vessels absorb less light than the curved ones. As for the blood perfusion, it is the mix-information which can be detected by LDI and LSI, and it may contain the information of diameter and depth. It is reported that if it decreases after V-PDT, the efficacy will be decent.

Conclusion and prospect This paper summarizes the current application of the non-invasive *in vivo* optical imaging technology in the diagnosis and treatment of PWS as well as the relationship between PWS lesion structure and V-PDT efficacy. By mastering the above information, the clinical doctors can develop an accurate and personalized V-PDT treatment of PWS and thus improve the therapeutic effects.

Key words medical optics; port wine stains; vascular-targeted photodynamic therapy; lesion structure; therapeutic effects